ChemComm

COMMUNICATION

View Article Online
View Journal | View Issue

Cite this: *Chem. Commun.*, 2021, **57**, 2661

Received 25th November 2020,
Accepted 22nd January 2021

DOI: 10.1039/d0cc07740b

rsc.li/chemcomm

Ribosome-mediated incorporation of fluorescent amino acids into peptides *in vitro*†

Joongoo Lee, ‡[a] Kevin J. Schwarz,‡[b] Hao Yu,[c] Antje Krüger,[a] Eric V. Anslyn,[d] Andrew D. Ellington,[e] Jeffrey S. Moore*[bf] and Michael C. Jewett*[a]

We report the design, chemical synthesis, and flexizyme-catalyzed transfer RNA (tRNA) acylation of a variety of fluorescent amino acids (FAAs). The fluorescent groups include pyrene, coumarin, nitrobenzoxadiazole, and fluorescein variants. We further demonstrate site-specific incorporation of the FAAs into peptides by the ribosome *in vitro* through genetic code reprogramming.

The site-specific incorporation of non-canonical amino acids (ncAAs) into peptides and proteins provides a path to bio-based products with new structures and functions.[1,2] To date, more than 200 α-L-ncAAs,[3,4] as well as β-,[5–7] long-chain carbon (γ-, δ-, ε-, and ζ-),[8] cyclic,[9,10] D-,[11] aliphatic,[12] aromatic,[12] aminobenzoic,[13] *N*-alkylated,[14] oligomeric,[15] and fluorescent[16,17] amino acid derivatives have been used in ribosome-mediated polymerization. These advances have led to new products, such as human therapeutics,[18] enzymes,[19] antibody–drug conjugates,[20] macrocyclic and peptidomimetic drugs,[21] and genetically encoded materials.[8,22–24] These innovations have also provided new ways to study protein structure, dynamics, localization, and post-translational modifications.[25]

The ability to introduce fluorescent groups on amino acids[26] is particularly powerful in studying proteins; such as, single-biomolecule spectroscopy where an amino acid-sized fluorescent reporter is required that can be precisely introduced into a protein without significant structural perturbations.[16,17] In addition, fluorophores can provide insights into protein conformational changes.[27] Labeling proteins with green fluorescent protein (GFP) on the N- and/or C-terminus is an alternative, but the large GFP derivatives can impact protein structure and function.[28] Thus, having access to a broad set of fluorescent amino acids (FAAs) for use in ribosome-mediated polymerization should facilitate both biochemical and cellular studies of protein structure and function.

While there have been multiple reports of introducing FAAs into proteins, those in cell-free, or *in vitro*, systems offer the opportunity to rapidly expand the FAA repertoire.[1,29,30] This is because cell-free systems offer a freedom of design for manipulating the level and identity of translational components and reagents.[1] So far, *in vitro* studies have leveraged chemical aminoacylation of FAA monomers to transfer RNA (tRNA) substrates. Chemical aminoacylation requires the cumbersome synthesis of 5′-phospho-2′-deoxyribocytidylylriboadenosine dinucleotide, ester coupling with the amino-acid substrate, and enzymatic ligation with a truncated tRNA. A variety of BODIPY-linked amino acids[31–33] have been previously incorporated into proteins with this approach. However, BODIPY monomers are bulky, and previous studies have had low incorporation efficiency.[34,35] Notably, chemical aminoacylations are not applicable to a wide variety of functional groups. This is because chemical aminoacylations are laborious and undesired chemical reactions with functional groups on the substrate of interest can occur if these groups are not properly protected. In addition, the tRNA-monomer substrates can give poor results in translation owing to the generation of a cyclic tRNA byproduct, which inhibits ribosomal peptide synthesis.[36]

Here, we set out to address these limitations to broaden the repertoire of FAAs used in molecular translation. The key idea was to explore if the flexizyme (Fx)-based genetic code reprogramming approach (aminoacyl-tRNA synthetase-like ribozymes)[37] could be used to charge α-L-amino acids containing fluorescent groups with shorter side chains than BODIDY, such as pyrene (**1**), coumarin (**2**–**4**), nitrobenzoxadiazole (**5**), and fluorescein (**6**) variants that absorb and emit light over a wide range of wavelengths (Fig. 1). These fluorescent groups were selected because they have not yet,

[a] *Department of Chemical and Biological Engineering and Center for Synthetic Biology, Northwestern University, Evanston, IL 60208, USA*
[b] *Department of Chemistry, University of Illinois at Urbana-Champaign, Urbana, 61801, IL, USA. E-mail: jsmoore@illinois.edu*
[c] *Departments of Chemical and Biomolecular Engineering, University of Illinois at Urbana-Champaign, Urbana, Illinois, 61801, USA*
[d] *Department of Chemistry and Biochemistry, University of Texas at Austin, Austin, 78712, TX, USA*
[e] *Department of Chemistry and Biochemistry, Institute for Cellular and Molecular Biology, University of Texas at Austin, Austin, 78712, TX, USA*
[f] *Beckman Institute for Advanced Science and Technology, University of Illinois at Urbana-Champaign, Urbana, Illinois 61801, USA*

† Electronic supplementary information (ESI) available. See DOI: 10.1039/d0cc07740b
‡ J. L. and K. J. S. contributed equally.

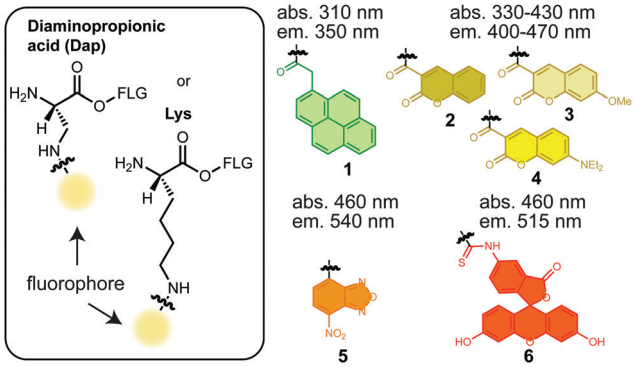

Fig. 1 Design of fluorescent non-canonical amino acids. We expand the substrate scope of ribosome-mediated incorporation to α-amino acids with a variety of fluorescent groups on the sidechain. We explore the specificity of the aminoacyl-tRNA synthetase-like ribozyme (flexizyme) and the translation machinery for 14 non-canonical fluorescent amino acids (FAAs) with different lengths of sidechain (Dap and Lys) and bulkiness of the fluorescent groups (**1–6**).

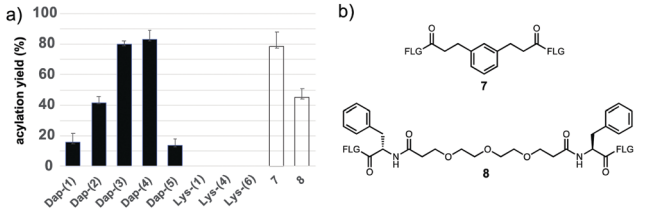

Fig. 2 Flexizyme-mediated charging of fluorescent amino acids (FAAs). (a) Relative yields of Fx-mediated acylation of FAAs on a tRNA mimic (microhelix). No Lys-FAA variants were successful, but modified substrates were (see b). Error bars show standard deviation of $n = 3$ independent experiments. (b) Two modified substrates bearing an extended carbon chain (**7**) and PEG units (**8**) were prepared and successfully charged to mihx (see a). It appears that multiple aromatics on a longer carbon sidechain increase the steric hindrance around the carbonyl group, thereby reducing the yield of tRNA charging. FLG:Fx pair used for acylation; Dap-**1**-CME:eFx, Dap-**2**-CME:aFx, Dap-**3**-CME:eFx, Dap-**4**-CME:aFx, Dap-**5**-DNB:aFx, **7**-CME:eFx, and **8**-CME:eFx.

to our knowledge, been directly charged to tRNA by Fx without using an auxiliary amino acid handle (*e.g.*, Phe)[38,39] or polymerized into a growing polypeptide chain by the ribosome using a cell-free protein synthesis platform. We first confirm Fx-mediated tRNA charging of the FAA substrates, and identify spatial constraints on length and bulkiness of the functional group of α-amino acids. Then, we demonstrate incorporation into peptides using an *in vitro* ribosome-mediated protein synthesis platform (PURExpress™) and characterize the peptides with mass spectrometry. Additionally, we successfully incorporate three FAAs consecutively into a peptide.

Since FAAs are bulky, we hypothesized that successful Fx-charging depends on sidechain length. Therefore, two amino acids (L-diaminopropionic acid (Dap) and L-Lys) with different sidechain lengths were initially used in this work (Fig. 1). We prepared and tested 14 FAA variants of the Fx-leaving groups (FLGs) including cyanomethylester (CME), dinitrobenzylester (DNB), and amino-derivatized benzylthioester (ABT) as these are all known as efficient leaving groups for Fx-mediated acylation. The substrates include Dap-**1**-CME;ABT, Dap-**2**-CME;DNB, Dap-**3**-CME, Dap-**4**-CME, Dap-**5**-CME;DNB;ABT, and Lys-**1**-CME;DNB, Lys-**4**-CME;DNB, Lys-**6**-DNB (see ESI,† for details).

In general, the FAA substrates were prepared in three steps: (i) coupling fluorophores to the Dap or Lys sidechain, (ii) esterification of carboxylate with a Fx leaving group, and (iii) Boc deprotection from the α-amine of Dap or Lys (Fig. S1 and S2, ESI†). To determine and optimize the tRNA acylation reaction conditions for the FAAs (Dap-**1** through Dap-**5**), we used a short tRNA mimic (22nt) called the microhelix tRNA (mihx) as the FAA acceptor. Yields of Fx-catalyzed acylation were determined by a densitometric analysis of RNA bands on an acidic polyacrylamide gel (pH 5.2, NaOAc) (Fig. S3, ESI†). All five Dap variants were charged to mihx by Fx (15–83% yields) (Fig. 2a). No Lys variants containing the same fluorescent groups (**1** and **4**) were charged on mihx (Fig. 2a). This was surprising since macromolecule foldamers linearly oligomerized along the amide backbone have been charged to tRNA by the Fx approach.[3,14,40] Hence, we sought to understand the limitations of Fx-catalyzed acylation of the Lys-based FAA substrates. To gain insights, we tested two additional substrates (3,3′-(1,3-phenylene)-dipropionic acid ($PhPA_2$, **7**) and Phe-$(PEG)_3$-Phe (**8**), Fig. 2b) bearing an extension along the main carbon backbone chain instead of on the branched carbon chain. The two substrates were charged to mihx (Fig. 2a and Fig. S3, ESI†). Our results are consistent with past literature[41] showing nucleophilic reactions to the carbonyl carbon of branched amino acid residues are challenging. Characteristic fluorescent spectra were observed in UV-Vis absorption spectroscopy for activated FAAs, such as Dap-**3**-CME and Dap-**5**-CME (Fig. S4, ESI†).

Using the conditions optimized from our mihx experiments, we performed the acylation reaction for tRNAs to be used in ribosome-mediated incorporation. The resulting tRNA-FAA complexes were ethanol-precipitated and then supplemented into a cell-free protein synthesis reaction. We used the PURExpress™ (ΔtRNA, Δaa) system, which contains a minimal set of components required for peptide synthesis. As a reporter peptide, we designed a T7 promoter-controlled plasmid (pJL1_StrepII_1) encoding a Streptavidin tag (WSHPQFEK) followed by a Ser codon and then a Thr codon. The product peptide sequence was thus **X**WSHPQFEKST or MWSHPQFEKS**X**, where **X** indicates the position to which a Fx-charged FAA is incorporated. For N-terminal incorporation, $tRNA^{fMet}$(CAU) was selected as the initiator tRNA, decoding the Met(AUG) codon of an mRNA, and a set of 9 amino acids (WSHPQFEK+T) was supplemented to the reaction. For C-terminal incorporation, $tRNA^{Pro1E2}$(GGU) previously engineered to efficiently incorporate ncAAs into polypeptides by the ribosome was selected,[42] and a separate set of 9 amino acids (M+WSHPQFEK) was used. GGU was selected as the anticodon because it decodes the Thr(ACC) codon in an mRNA, which is excluded from the Strep-tag. This avoided aminoacylation of Thr onto the corresponding endogenous tRNA, eliminating competition with the Fx-charged tRNA in the PURExpress™ reaction. The reactions were incubated at 37 °C for 3 h. The resulting peptides were purified using Strep-Tactin-coated

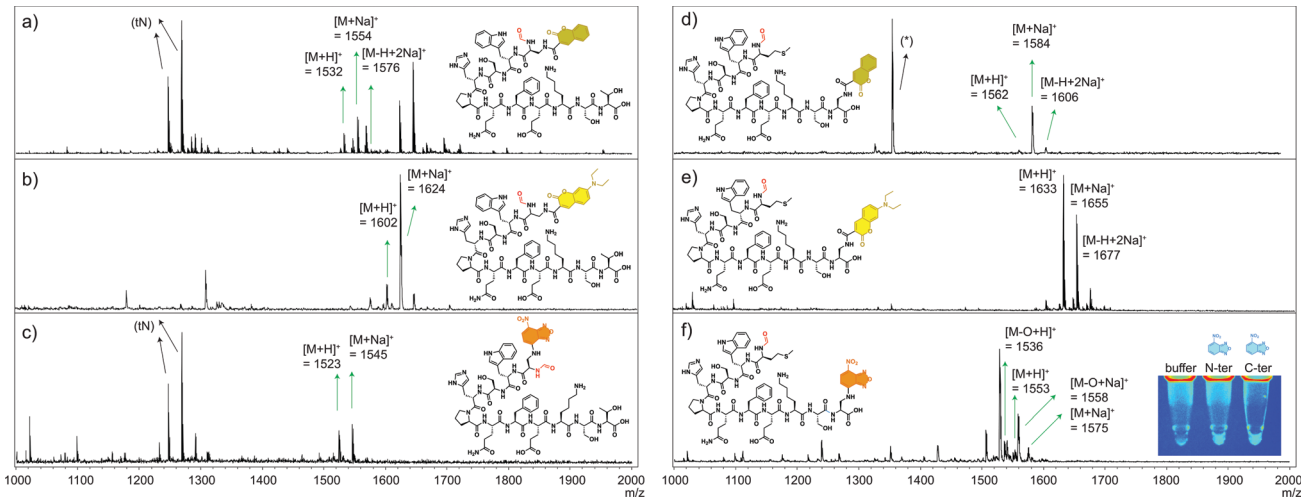

Fig. 3 Ribosomal incorporation of FAAs. The substrates were charged to either $tRNA^{fMet}$(CAU) or $tRNA^{Pro1E2}$(GGU) for N- or C-terminal incorporation and supplemented into the PURExpress™ system to produce a short model peptide (Strep tag). The theoretical masses for the peptides are (a) $[M+H]^+$ = 1532; $[M+Na]^+$ = 1554; $[M-H+2Na]^+$ = 1576, (b) $[M+H]^+$ = 1603; $[M+Na]^+$ = 1625, (c) $[M+H]^+$ = 1523; $[M+Na]^+$ = 1545, (d) $[M+H]^+$ = 1562; $[M+Na]^+$ = 1584, $[M-H+2Na]^+$ = 1606, (e) $[M+H]^+$ = 1633; $[M+Na]^+$ = 1655; $[M-H+2Na]^+$ = 1677, and (f) $[M+H]^+$ = 1553; $[M+Na]^+$ = 1575; $[M-O+H]^+$ = 1537, $[M-O+Na]^+$ = 1559, respectively. The peaks denoted with tN correspond to a truncated peptide not bearing the target FAA at the N-terminal codon. tN: $[M+H]^+$ = 1246; $[M+Na]^+$ = 1268. The peaks marked with an asterisk ($[M+H]^+$ = 1334; $[M+Na]^+$ = 1356) were unidentified. The UV light-exposed peptide containing Dap-**5** either at N- or C-terminus showed fluorescent characteristics (inset in f). Data are representative of n = 3 independent experiments.

magnetic beads (IBA), and denatured with 0.1% SDS in water at 95 °C for 2 min. We then determined the N- and C-terminal incorporation of the FAAs into the Strep-tag peptide by mass spectrometry (MALDI-TOF). For all reactions supplemented with cognate tRNA complexes of Dap-**2**, Dap-**4**, Dap-**5**, **7**, and **8**, we observed peaks corresponding to the theoretical masses of the peptides that contain the FAAs either at the N- or C-terminus (Fig. 3 and Fig. S5, ESI†). Of note, the single incorporation efficiency (%) at the N-terminus (Dap-**2**: 9%, Dap-**4**: 67%, Dap-**5**: 24%) and C-terminus (Dap-**2**: 34%, Dap-**4**: 81%, Dap-**5**: 29%) suggests that the ribosomal incorporation of FAA may be limited by the acylation yield. We carried out additional experiments to address the low FAA incorporation efficiency using EF-P, a bacterial translation factor that can prevent ribosome stalling. Unfortunately, FAA incorporation efficiency was not enhanced by the addition of EF-P (Fig. S6, ESI†).

Next, we investigated the fluorescent properties of the resulting peptides for potential applications of FAAs. To visualize the fluorescent characteristics, we exposed the peptides to UV light (560 nm) on a Bio-Rad gel imager (Gel Doc™ XR). We found that only the peptides containing Dap-**5** (Fig. 3c and f) showed fluorescent characteristics from the excitation light source. This was expected since the wavelength of the exposed light was longer than the wavelength that Dap-**2** and Dap-**4** absorb (330–360 nm, Fig. 1) and therefore, the intensity of emitted light from a single Dap-**2** or **4** was not sufficient to be detected on the equipment.

We next tested multiple incorporations of FAAs into peptides using coumarin variants. We repeated the PURExpress™ reaction described above with Dap-**3** acylated onto three different tRNAs (Pro1E2(GGU), GluE2(GAU), GluE2(GGC)), respectively, using the same set of amino acids to express Strep-tag, but supplemented with different plasmids (pJL1_Strep_2 and pJL1_Strep_3, see plasmid map in ESI†) that contain additional codons decoding Thr(ACC), Ile(AUC), and Ala(GCC) at the C-terminus of the Strep-tag. The MALDI spectra (Fig. 4a–c) yielded only a single peak corresponding to the theoretical mass of peptides with MWSHPQFEKS-(Dap-**3**)$_n$ (where n = 1–3), indicating that the

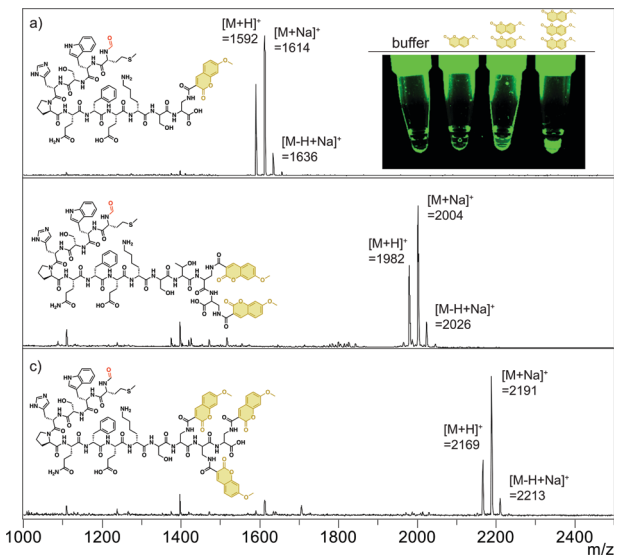

Fig. 4 Incorporation of multiple FAAs into a peptide. Three Dap-**3**s were consecutively incorporated into a peptide with three different engineered tRNA variants decoding the Thr(ACC), Ile(AUC), and Ala(GCC) codons on mRNA. The resulting peptide fluorescence intensity was dependent on the number of incorporated FAAs (inset). The theoretical masses for the peptides are (a) $[M+H]^+$ = 1592; $[M+Na]^+$ = 1614; $[M-H+2Na]^+$ = 1636, (b) $[M+H]^+$ = 1982; $[M+Na]^+$ = 2004; $[M-H+2Na]^+$ = 2026, and (c) $[M+H]^+$ = 2169; $[M+Na]^+$ = 2191; $[M-H+2Na]^+$ = 2213. Data are representative of n = 3 independent experiments.

ribosome can consecutively polymerize multiple FAAs with bulky aromatic groups into the C-terminus of a peptide in high efficiency. Notably, peptides containing more than two Dap-**3**s showed more intense fluorescent characteristic compared to peptides with a single Dap-**2**, **3**, or **4** under the same light exposure condition (inset in Fig. 4a).

Finally, we assessed peptides yields. We quantified the yield of the peptides shown in the inset of Fig. 3f and 4a by comparing the fluorescence intensity of the figures to the intensity of the FAAs (Dap-**3** and Dap-**5**) diluted to several known concentrations (Fig. S7, ESI†). Overall, the yields we obtained were ~520 ng (330 nmol) and ~116 ng (75 nmol), for the peptide containing a single Dap-**3** and Dap-**5** in a 10 μL reaction volume, respectively, which is comparable with previous works in PURExpress™.[43]

In summary, our work expands the range of ncAAs for use in genetic code reprogramming by demonstrating Fx-mediated charging of FAAs onto tRNAs and their incorporation into peptides by the ribosome. Our work has several key features. First, we observed that acylation efficiency is largely dependent on the size of the fluorescent group and the length of the amino acid sidechain that links to the fluorescent group. Second, we successfully demonstrated consecutive incorporation of FAAs into a peptide with high efficiency using the wildtype ribosome. Third, we produced a set of peptides with different fluorescence intensities that increases with the number of codons for FAA incorporation assigned in an mRNA. Based on our observations, a high incorporation efficiency of FAAs can be obtained when a short side chain α-amino acid is used and the acylation efficiency is higher than 40%. Looking forward, further optimizations can improve incorporation efficiencies. Taken together, we expect this work to open new possibilities in synthetic and chemical biology applications, such as protein labelling, sensing, and imaging.

JL, KJS, HY, AK, EVA, ADE, JSM, and MCJ conceived and designed the research. JL, KJS, HY, and AK performed experiments. All authors wrote and edited the manuscript. JS M and MCJ supervised this study. This work was supported by the Army Research Office Grant W911NF-16-1-0372. This work made use of IMSERC at Northwestern University.

Conflicts of interest

MCJ, JSM, JL, and KJS are co-inventors on the US provisional patent that incorporates discoveries described in this manuscript. All other authors declare no competing interests.

References

1 M. J. Hammerling, A. Kruger and M. C. Jewett, *Nucleic Acids Res.*, 2020, **48**, 1068–1083.
2 P. Arranz-Gibert, K. Vanderschuren and F. J. Isaacs, *Curr. Opin. Chem. Biol.*, 2018, **46**, 203–211.
3 J. M. Rogers and H. Suga, *Org. Biomol. Chem.*, 2015, **13**, 9353–9363.
4 T. Mukai, M. J. Lajoie, M. Englert and D. Soll, *Annu. Rev. Microbiol.*, 2017, **71**, 557–577.
5 T. Fujino, Y. Goto, H. Suga and H. Murakami, *J. Am. Chem. Soc.*, 2016, **138**, 1962–1969.
6 C. Melo Czekster, W. E. Robertson, A. S. Walker, D. Soll and A. Schepartz, *J. Am. Chem. Soc.*, 2016, **138**, 5194–5197.
7 T. Katoh and H. Suga, *J. Am. Chem. Soc.*, 2018, **140**, 12159–12167.
8 J. Lee, K. J. Schwarz, D. S. Kim, J. S. Moore and M. C. Jewett, *Nat. Commun.*, 2020, **11**, 4304.
9 J. Lee, R. Torres, M. Byrom, A. D. Ellington and M. C. Jewett, *Chem. Commun.*, 2020, **56**, 5597–5600.
10 T. Katoh and H. Suga, *J. Am. Chem. Soc.*, 2020, **142**, 4965–4969.
11 T. Katoh, K. Tajima and H. Suga, *Cell Chem. Biol.*, 2017, **24**, 46–54.
12 J. Lee, K. E. Schwieter, A. M. Watkins, D. S. Kim, H. Yu, K. J. Schwarz, J. Lim, J. Coronado, M. Byrom, E. V. Anslyn, A. D. Ellington, J. S. Moore and M. C. Jewett, *Nat. Commun.*, 2019, **10**, 5097.
13 T. Katoh and H. Suga, *J. Am. Chem. Soc.*, 2020, **142**, 16518–16522.
14 T. Kawakami, T. Ishizawa and H. Murakami, *J. Am. Chem. Soc.*, 2013, **135**, 12297–12304.
15 Y. Goto and H. Suga, *J. Am. Chem. Soc.*, 2009, **131**, 5040–5041.
16 D. Summerer, S. Chen, N. Wu, A. Deiters, J. W. Chin and P. G. Schultz, *Proc. Natl. Acad. Sci. U. S. A.*, 2006, **103**, 9785–9789.
17 J. Wang, J. Xie and P. G. Schultz, *J. Am. Chem. Soc.*, 2006, **128**, 8738–8739.
18 D. Raucher and J. S. Ryu, *Trends Mol. Med.*, 2015, **21**, 560–570.
19 J. Despanie, J. P. Dhandhukia, S. F. Hamm-Alvarez and J. A. MacKay, *J. Controlled Release*, 2016, **240**, 93–108.
20 Z. Dai, X. N. Zhang, F. Nasertorabi, Q. Cheng, J. Li, B. B. Katz, G. Smbatyan, H. Pei, S. G. Louie, H. J. Lenz, R. C. Stevens and Y. Zhang, *Sci Adv.*, 2020, **6**, eaba6752.
21 T. Katoh, T. Sengoku, K. Hirata, K. Ogata and H. Suga, *Nat. Chem.*, 2020, **12**, 1081–1088.
22 A. A. Vinogradov, M. Shimomura, Y. Goto, T. Ozaki, S. Asamizu, Y. Sugai, H. Suga and H. Onaka, *Nat. Commun.*, 2020, **11**, 2272.
23 O. Ad, K. S. Hoffman, A. G. Cairns, A. L. Featherston, S. J. Miller, D. Soll and A. Schepartz, *ACS Cent. Sci.*, 2019, **5**, 1289–1294.
24 S. A. Costa, D. Mozhdehi, M. J. Dzuricky, F. J. Isaacs, E. M. Brustad and A. Chilkoti, *Nano Lett.*, 2019, **19**, 247–254.
25 J. W. Chin, *Nature*, 2017, **550**, 53–60.
26 M. Kitamatsu, M. Futami and M. Sisido, *Chem. Commun.*, 2010, **46**, 761–763.
27 S. M. Huang, F. Yang, B. Y. Cai, Q. T. He, Q. Liu, C. X. Qu, M. J. Han, W. Kong, Y. L. Jia, F. Li, X. Yu, J. P. Sun and J. Wang, *Anal. Chem.*, 2019, **91**, 14936–14942.
28 J. Zhang, R. E. Campbell, A. Y. Ting and R. Y. Tsien, *Nat. Rev. Mol. Cell Biol.*, 2002, **3**, 906–918.
29 A. D. Silverman, A. S. Karim and M. C. Jewett, *Nat. Rev. Genet.*, 2020, **21**, 151–170.
30 R. W. Martin, B. J. Des Soye, Y. C. Kwon, J. Kay, R. G. Davis, P. M. Thomas, N. I. Majewska, C. X. Chen, R. D. Marcum, M. G. Weiss, A. E. Stoddart, M. Amiram, A. K. Ranji Charna, J. R. Patel, F. J. Isaacs, N. L. Kelleher, S. H. Hong and M. C. Jewett, *Nat. Commun.*, 2018, **9**, 1203.
31 D. Kajihara, R. Abe, I. Iijima, C. Komiyama, M. Sisido and T. Hohsaka, *Nat. Methods*, 2006, **3**, 923–929.
32 I. Iijima and T. Hohsaka, *ChemBioChem*, 2009, **10**, 999–1006.
33 T. Ohtsuka, S. Neki, T. Kanai, K. Akiyoshi, S. I. M. Nomura and T. Ohtsuki, *Anal. Biochem.*, 2011, **418**, 97–101.
34 K. Wang, H. Neumann, S. Y. Peak-Chew and J. W. Chin, *Nat. Biotechnol.*, 2007, **25**, 770–777.
35 H. Neumann, K. Wang, L. Davis, M. Garcia-Alai and J. W. Chin, *Nature*, 2010, **464**, 441–444.
36 J. Wang, M. Kwiatkowski and A. C. Förster, *J. Am. Chem. Soc.*, 2016, **138**, 15587–15595.
37 H. Murakami, A. Ohta, H. Ashigai and H. Suga, *Nat. Methods*, 2006, **3**, 357–359.
38 Y. Yamagishi, H. Ashigai, Y. Goto, H. Murakami and H. Suga, *ChemBioChem*, 2009, **10**, 1469–1472.
39 N. Terasaka, G. Hayashi, T. Katoh and H. Suga, *Nat. Chem. Biol.*, 2014, **10**, 555–557.
40 J. M. Rogers, S. Kwon, S. J. Dawson, P. K. Mandal, H. Suga and I. Huc, *Nat. Chem.*, 2018, **10**, 405–412.
41 T. M. Hackeng, J. H. Griffin and P. E. Dawson, *Proc. Natl. Acad. Sci. U. S. A.*, 1999, **96**, 10068–10073.
42 T. Katoh, Y. Iwane and H. Suga, *RNA Biol.*, 2018, **15**, 453–460.
43 C. Tuckey, H. Asahara, Y. Zhou and S. Chong, *Curr. Protoc. Mol. Biol.*, 2014, **108**(1), 16.31.1–16.31.22.

